Electric Power Systems Research 213 (2022) 108458

Contents lists available at ScienceDirect

Electric Power Systems Research

journal homepage: www.elsevier.com/locate/epsr

Enhancing topology error detection via multiple measurement scans

Bilgehan Donmez [*], Ali Abur

Department of Electrical and Computer Engineering, Northeastern University, Boston, USA

ARTICLE INFO

Keywords:
Bus-branch
Measurement scan
Node-breaker
State estimation
Topology error

ABSTRACT

In today's energy management systems, the network model being fed into state estimation (SE) is assumed to be free of topology errors. In this conventional approach, bus-branch (BB) models are created as electrical equivalents of the actual network. If any topology error goes undetected while forming BB models, the subsequent SE solution will be either biased or divergent. To deal with topology errors, in this paper, a topology tracking method, using the detailed node-breaker (NB) models, is formulated. In large systems, it is computationally intensive to run SE and the following bad data tests. Therefore, SE analysis is carried out every few minutes, which is less frequent than the measurement updates (every few seconds). Since contingencies develop quickly (less than a second), the switching device flows in a few substations can change significantly from one measurement scan to the next. To identify the substation most impacted by the event, an efficient SE procedure based on the Lasso (least absolute shrinkage and selection operator) method is developed. Then, the correct topology is obtained by running a localized SE centered around the identified substation. The efficacy of the proposed approach is demonstrated both in a small 13-bus and a large 300-bus IEEE test cases.

1. Introduction

State estimation (SE) was developed and commercialized in 1970s. During early days, computational limitations necessitated a pre-SE program called topology processor to reduce actual substation layouts to bus-branch (BB) equivalents [1,2]. This way the network size was kept at computationally manageable levels. In the ensuing decades, significant improvements that focus on SE's convergence and accuracy have been recorded, but no major advances on how the network models are constructed have been made. Even the latest commercial energy management systems rely on the same topology processing techniques introduced in 1970s.

Similarly, for post-processing SE results, bad data detection tests have become quite capable in detecting and eliminating measurement errors. However, the success of these bad data tests are still limited by the accuracy of the network topology created by the topology processor. With the recent advances in computational capabilities, it is now possible to replace bus-branch equivalents with detailed substation representations, including all nodes and breakers. The use of these detailed models, called node-breaker (NB) models, will allow detection of not only bad data but also topology errors.

To deal with topology errors, early research identified the need to incorporate circuit breaker (CB) flows, which are the real and reactive power flows through a CB, into SE formulation as new state variables [3–5]. It was shown that by estimating CB flows, changes in CB statuses (open/closed) can be detected, revealing topology errors. Building on this idea, several interesting papers offered ways to handle topology errors [6–9]. Also, a commercial application of an SE algorithm with topology error detection capability was presented in [10]. Most of these earlier approaches relied on a two-step process where BB-models are used first to find the general location of the topology error. Then, NB models are incorporated only for a few substations to identify the changes in network topology. These approaches are shown to be successful as long as the SE does not fail in the first step.

In more recent research, approaches that modify the conventional weighted least squares (WLS) SE to capture CB-flow states have been proposed [11–15]. In most of these papers, the WLS objective function is extended by adding either a quadratic or linear term related to a priori information of the CB-flow states. These approaches are shown to be effective either for a linear SE formulation or applications to small networks. However, limited insights are given for their applicability to large systems using nonlinear SCADA measurements.

On the distribution side, topology detection has also received significant attention lately. Although there are many interesting references, only the approach in [16] is similar to our proposed algorithm in its utilization of the Lasso, a method for regression shrinkage and selection [17].

To address the scalability issues of topology error detection, a new SE framework using NB models is presented in [18]. Through

* Corresponding author.
E-mail addresses: donmez.b@northeastern.edu (B. Donmez), abur@ece.neu.edu (A. Abur).

https://doi.org/10.1016/j.epsr.2022.108458
Received 2 October 2021; Received in revised form 10 April 2022; Accepted 2 July 2022
Available online 3 August 2022
0378-7796/

utilization of parallel processing and zone-partitioning, it is shown that joint topology and state estimation is feasible for large systems. In this paper, building on the work of [18], an alternative, computationally efficient topology tracking method is proposed. Considering an SE cycle (SE solution and its subsequent bad data tests) is typically executed once every few minutes, contingencies (e.g., outages, faults) can still develop in between two SE runs. As new information streams (measurement scans) come in every few seconds, they can be exploited to detect contingencies, without having to wait for the next SE run. This approach is used in the proposed method to detect a topology change in a given substation. Then, a localized SE encompassing the suspect substation (and a small number of its neighbors) is run to identify the correct topology.

The main contribution of the proposed method is that it offers efficient topology tracking in the time window between consecutive SE cycles (typically 3 to 5 min). To detect topology errors from one measurement scan to the next, a modified SE based on the Lasso is formulated. In case of contingencies, the few nonzero states obtained from the Lasso solution pinpoint the substation that experienced the topology change. Using this location information, a small network including the suspect substation and a small number of its neighbors are carved out. Then, the correct topology is revealed running SE on this small network. Since this localized area is a fraction of the whole system, this procedure is computationally manageable and can be executed at each measurement scan to catch contingencies.

The paper is organized as follows. A short overview of NB modeling and least absolute value (LAV) SE are given in Sections 2 and 3, respectively. The sparse estimation algorithm is developed in Section 4. The viability of the proposed method is demonstrated via simulations in Section 5.

2. SE formulation for node-breaker modeling

The main difference of SE formulation in NB models compared with conventional BB models is that the real and reactive power flows through CBs become additional system states [4,5]. Assuming the system has n voltage states and l CB-flow states, the measurement equations in NB models can be written as:

$$\boldsymbol{z} = h(\boldsymbol{x}, \boldsymbol{f}) + \boldsymbol{e} \tag{1}$$

where, $\boldsymbol{x} \in \mathbb{R}^n$ and $\boldsymbol{f} \in \mathbb{R}^l$ are the vectors of voltage states (magnitudes and angles) and CB-flow states (real and reactive power flows through CBs), respectively; $\boldsymbol{z}$ and $\boldsymbol{e}$ represent the measurements and their Gaussian errors; $h(\boldsymbol{x}, \boldsymbol{f})$ is the nonlinear function relating the system states to measurements.

In addition to the common measurements (branch power flows, bus power injections and bus voltage magnitudes) used in conventional SE, a certain number of CB flows needs to be included for observability of the new system states. Fortunately, NB modeling yields many free (virtual and pseudo) measurements based on KCL equations within a substation. Utilization of these equations reduce the number of CB-flow measurements needed for observability. The pseudo measurements correspond to the real and reactive power injection equations for nodes with no load or generation injections, i.e., they are always equal to zero. The virtual measurements consist of zero-voltage-drops across closed CBs and zero-current-flows through open CBs. These constraints need to be modeled as soft constraints to allow SE to correct the CB statuses in case of topology errors. On the other hand, pseudo measurements are modeled as hard constraints since they are always true regardless of the actual topology of the system. Similar to (1), KCL-based equations can be grouped as a set of nonlinear equations:

$$c(\boldsymbol{x}, \boldsymbol{f}) = \boldsymbol{0} \tag{2}$$

where, $c(\boldsymbol{x}, \boldsymbol{f})$ is the nonlinear function representing the constraints. An example of all measurement types and constraints for a breaker-and-a-half substation is shown in Fig. 1.

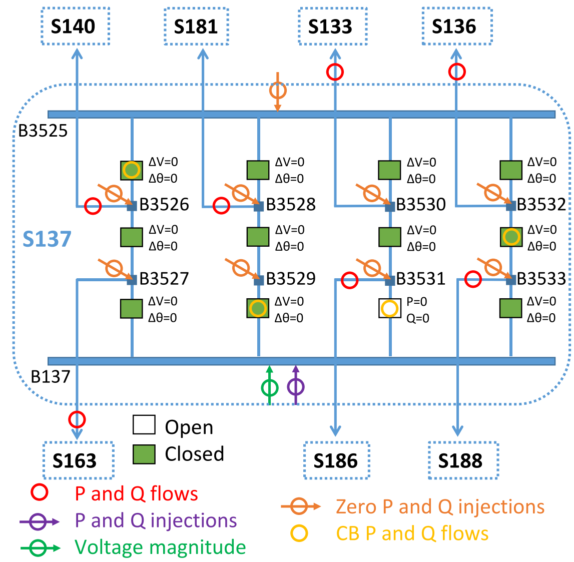

Fig. 1. Measurements in a breaker-and-a-half substation.

As shown by the yellow circles, only four CB-flow pairs are needed for CB-flow state observability. Four digit bus numbers (BXXXX) and three digit substation numbers (SXXX) are employed to allow modeling hundreds of substations and thousands of buses.

To ensure NB models are observable and free of critical measurements, two optimal measurement placement algorithms (one for observability and the other for critical measurement elimination) are formulated in [18]. It is shown that, rather than the conventional WLS, SE formulations suitable for handling large number of constraints are necessary for using NB models. The two common alternatives to WLS are LAV and Hachtel SE. Only LAV SE is described in the rest of this paper since it is computationally advantageous in the presence of multiple bad data and/or topology errors. Details of an Hachtel SE implementation and its comparison with LAV can be found in [18].

3. LAV SE formulation

LAV SE is formulated as l_1 optimization, where the objective is to minimize the sum of the absolute values of measurement residuals. The objective function J_L is written as:

$$J_L(\boldsymbol{x}, \boldsymbol{f}) = \sum_{i=1}^{m+s} \left| z_i - u_i(\boldsymbol{x}, \boldsymbol{f}) \right| \tag{3}$$

where m and s represent the number of measurements and equality constraints, respectively; and

$$u(\boldsymbol{x}, \boldsymbol{f}) = \begin{bmatrix} h(\boldsymbol{x}, \boldsymbol{f}) \\ c(\boldsymbol{x}, \boldsymbol{f}) \end{bmatrix}. \tag{4}$$

The nonlinear equations in $u(\boldsymbol{x}, \boldsymbol{f})$ can be approximated by a first order Taylor series to yield the following linearized version of the LAV problem:

$$\text{minimize} \quad J_L(\boldsymbol{x}^k, \boldsymbol{f}^k) = \sum_{i=1}^{m+s} \left| r_i^k \right| \tag{5}$$

$$\text{subject to} \quad \boldsymbol{r}^k = \begin{bmatrix} \Delta \boldsymbol{z}^k \\ \Delta \boldsymbol{c}^k \end{bmatrix} - \begin{bmatrix} \boldsymbol{H} & \boldsymbol{M} \\ \boldsymbol{H}_c & \boldsymbol{M}_c \end{bmatrix} \begin{bmatrix} \Delta \boldsymbol{x}^k \\ \Delta \boldsymbol{f}^k \end{bmatrix} \tag{6}$$

where:

- $\boldsymbol{r}^k = \boldsymbol{z} - u(\boldsymbol{x}^k, \boldsymbol{f}^k)$ is the measurement residual vector at kth iteration,
- $\Delta \boldsymbol{z}^k = \boldsymbol{z} - h(\boldsymbol{x}^k, \boldsymbol{f}^k)$, $\Delta \boldsymbol{c}^k = \boldsymbol{0} - c(\boldsymbol{x}^k, \boldsymbol{f}^k)$,

- $\boldsymbol{H} = \frac{\partial h}{\partial \boldsymbol{x}}$ at $\boldsymbol{x}^k$, $\boldsymbol{H}_c = \frac{\partial c}{\partial \boldsymbol{x}}$ at $\boldsymbol{x}^k$,
- $\boldsymbol{M}$ and $\boldsymbol{M}_c$ are the measurement to CB-flow incidence matrices,
- $\Delta \boldsymbol{x}^k = \boldsymbol{x} - \boldsymbol{x}^k$, $\Delta \boldsymbol{f}^k = \boldsymbol{f} - \boldsymbol{f}^k$.

Then, linear programming can be used to iteratively minimize the objective function as outlined in [18].

4. Error detection via consecutive measurement scans

Utilization of multiple measurement scans are shown to be effective in solving different SE problems before. For example, in [19], multiple scans were leveraged to improve measurement redundancy. Another example is given in [20], where authors use consecutive measurement sets to enhance parameter error detection capability. Similarly, in this paper, back-to-back measurement data streams are exploited to detect topology changes.

Remark 1 (*Impact of Topology Changes on System States*). Since the time interval between two scans is short (a few seconds at most), the load and generation would have little to no change unless a contingency/fault happens. Thus, during normal operation, most of the measurements will have negligible deviations from one scan to the next. On the other hand, when faults happen, protective devices (e.g., circuit breakers) operate quickly (within a few cycles) to clear a fault, yielding a new network topology. As a consequence, states in a few substations impacted by the topology change would have larger deviations than other states.

To detect topology changes, the difference between two measurement sets are examined. Using subscripts 1 and 2 to represent two consecutive measurement scans, the following linearized equations are written:

$$\begin{bmatrix} \boldsymbol{H} \\ \boldsymbol{H}_c \end{bmatrix} (\Delta \boldsymbol{x}_2 - \Delta \boldsymbol{x}_1) + \begin{bmatrix} \boldsymbol{M} \\ \boldsymbol{M}_c \end{bmatrix} (\Delta \boldsymbol{f}_2 - \Delta \boldsymbol{f}_1) + \boldsymbol{e} = \Delta \boldsymbol{z}_2 - \Delta \boldsymbol{z}_1. \tag{7}$$

Combining the terms to simplify the notation, where $\delta \boldsymbol{x} = \boldsymbol{x}_2 - \boldsymbol{x}_1$, $\delta \boldsymbol{f} = \boldsymbol{f}_2 - \boldsymbol{f}_1$ and $\delta \boldsymbol{z} = \Delta \boldsymbol{z}_2 - \Delta \boldsymbol{z}_1$, (7) becomes:

$$\begin{bmatrix} \boldsymbol{H} & \boldsymbol{M} \\ \boldsymbol{H}_c & \boldsymbol{M}_c \end{bmatrix} \begin{bmatrix} \delta \boldsymbol{x} \\ \delta \boldsymbol{f} \end{bmatrix} + \boldsymbol{e} = \delta \boldsymbol{z} \tag{8}$$

$$\boldsymbol{D}\ \boldsymbol{g} + \boldsymbol{e} = \delta \boldsymbol{z} \tag{9}$$

where $\boldsymbol{H}$ and $\boldsymbol{M}$ are augmented to form the $\boldsymbol{D}$ matrix, and $\delta \boldsymbol{x}$ and $\delta \boldsymbol{f}$ are appended to form the joint state vector $\boldsymbol{g}$.

Remark 2 (*Identifying the Substation with the Topology Error*). When a topology error emerges between two consecutive scans, it will impact most of the system states. Per Remark 1, a few entries of $\boldsymbol{g}$ closest to the topology error would have larger deviations. Applying a least-squares fit to (9) would reveal the changes in $\boldsymbol{g}$, but this solution would not be sparse. Instead, to narrow down the source of the topology error to a single substation, the least-squares fit can be regularized by introducing an l_1 penalty. This approach (the Lasso method) reduces the number of nonzeros in $\boldsymbol{g}$ to only a few significant ones (pointing to the substation with the topology error).

To implement the Lasso method, the following objective function including an l_1 penalty is written as:

$$\boldsymbol{g} := \underset{\boldsymbol{g}}{\operatorname{argmin}} \|\delta \boldsymbol{z} - \boldsymbol{D}\ \boldsymbol{g}\|_2^2 + \lambda \|\boldsymbol{g}\|_1 \tag{10}$$

where λ is the tuning parameter. If λ is zero, then the problem turns into a regular WLS estimation. Conversely, for a large enough λ, the solution will force all states to zero. By tuning λ, the solution of (10) can be limited to have only a few nonzeros, yielding the states of the substation corresponding to the topology change. The details of the Lasso method can be found in [17]. For simulations in Section 5, the tuning of λ is handled by an off-the-shelf solver, i.e., Matlab's Lasso function [21].

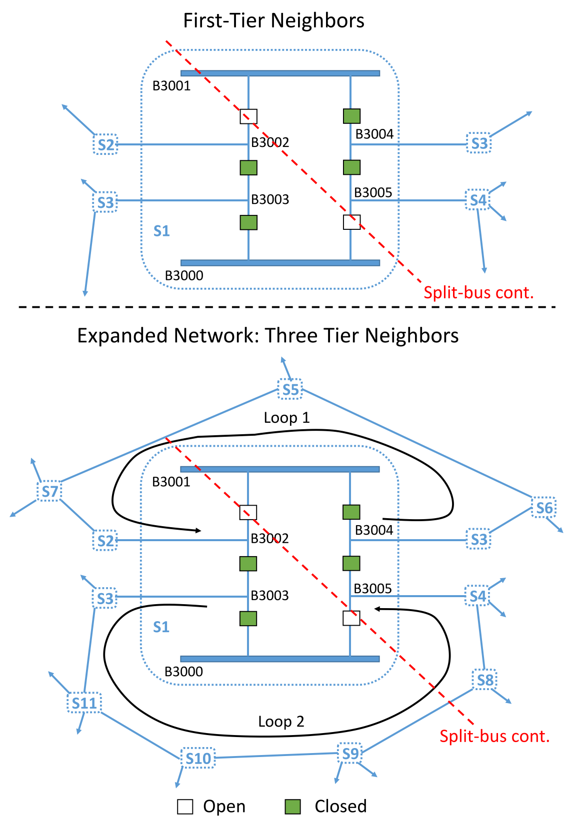

Fig. 2. Merging islands in case of a split-bus contingency in Sub. 1.

Although the Lasso solution can uncover the substation with the topology errors, identifying the details of the error requires further analysis. Since the error is localized to the substation identified by Lasso, there is no need to run SE on the whole NB model. Instead, a computationally efficient approach is to run analysis on a small network including the suspect substation and a few of its neighbors. The key requirements in setting up this small network is that it needs to be a single, observable island.

Remark 3 (*Forming a Small Network Around the Suspect Substation*). While forming a small network encircling the suspect substation, it is important to check observability to ensure the network created is a single, observable island. In addition, when a contingency electrically split a substation, it is necessary to enlarge the network to form a loop electrically connecting the split parts of the substation.

The formation of this small network can be done in a systematic manner, e.g., approaches based on numerical/graphical observability analysis or graph theory methods. Alternatively, a practical, ad hoc approach is to keep growing the network by including neighbors of the suspect substation until observability is achieved. In most cases, capturing two- or three-tier neighbors of the suspect substation would be sufficient to form an observable island. Note that in some cases, such as split-bus contingencies on radial sections, it might not be possible to merge islands for split-bus contingencies. Further analysis of error detectability and development of a systematic approach for island formation is left for future work.

An example of island formation around the suspect substation is illustrated in Fig. 2, where using only the first-tier neighbors creates two islands after the split-bus contingency (represented by the red dashed line). By adding additional tiers, loops can be formed connecting the

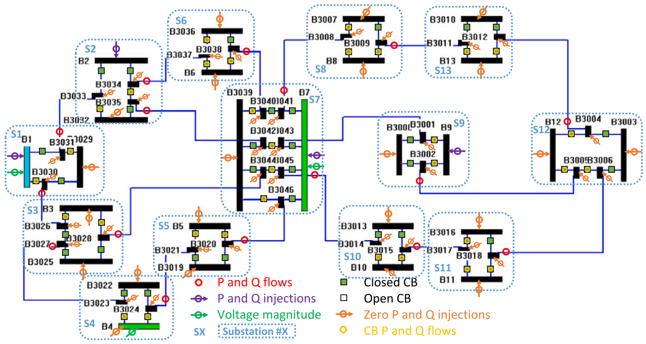

Fig. 3. Node-breaker representation of 13 bus system.

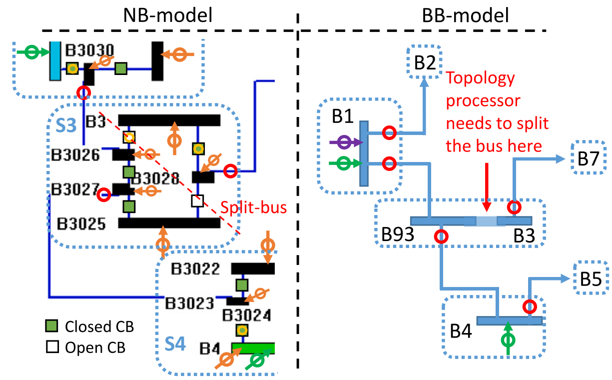

Fig. 4. Split-bus contingency at Substation #3 in NB and BB models.

two halves of Sub. 1 through its neighbors. A single loop would be sufficient to merge the split halves into a single observable island.

Once a small system around the identified substation is formed, LAV SE, as formulated in (5) and (6), and its ensuing bad data and CB-flow tests (the formulations of these tests can be found in [18]) are executed to reveal the correct system topology. To run SE in this small island, if no phasor measurement units (PMUs) exist, a fictitious voltage angle measurement can be placed on any one of the buses as a reference PMU to make the Jacobian matrix full rank. Alternatively, the conventional option is to delete one of the columns of the Jacobian matrix to retain observability.

5. Simulations

The proposed algorithm is tested on two different systems: (1) 13-bus system given in [22] and (2) the NB version of the IEEE 300-bus system from [18]. The 13-bus system is modified to convert each bus into actual substations with breakers as shown in Fig. 3. Power Education Toolbox (PET) is used to build the NB model [23]. Depending on the number of lines incident to a substation, either breaker-and-a-half, double-bus-double-breaker or ring-bus configurations are chosen. The load and generation are left in their original 13 buses and all other buses are modeled as zero-injection buses with 4 digit bus numbers. The total number of buses and circuit breakers in the NB model come out to 60 and 62, respectively.

For the measurement design, optimal meter placement algorithms described in [18] are used to add 32 CB-flow measurements. All original measurements from [22] are kept. In addition, KCL-based zero-voltage-drop (for closed breakers) and zero-power-flow (for open breakers) equations are added as virtual measurements, i.e., soft constraints. Zero-injection measurements are modeled as hard constraints since they are perfectly satisfied. Gaussian error is added to all measurements coming from a powerflow solution. Zero mean and 0.001/0.005 pu standard deviation are assumed for virtual/regular measurements. The slack variables for zero-injection measurements are set to zero to turn them into hard constraints in the linear programming implementation in LAV SE.

5.1. Application of the algorithm on the 13-bus system

To demonstrate the effectiveness of the proposed approach, a split-bus contingency is applied to Substation #3 (Sub. 3) as shown in Fig. 4. Any contingency that electrically splits a substation into two parts creates a major convergence issue for BB models until topology processor generates a new bus configuration. Before utilizing the NB model, SE is run first on the BB model to demonstrate its inability to identify topology errors.

Assuming the topology error has not had a chance to update the BB model by expanding Sub. 3 with a new bus, the SE ends up running with the incorrect electrical model. Running LAV SE with good measurements but erroneous network model yields conforming bad data as shown in Table 1. All three real flow measurements incident to Sub. 3 come out as bad data since their normalized residuals are greater than 3. In LAV SE, any measurements with nonzero residuals correspond to rejected measurements; the ones that have normalized residuals greater than 3 standard deviations indicate bad data. Reviewing the results presented in Table 1, an experienced system operator might be able to deduce that a topology error exists at Sub. 3. However, it would not be possible to figure out the correct statuses of CBs based on this BB model.

Next, the proposed algorithm is tested on the NB version of the 13-bus system given in Fig. 3. The Lasso function in Matlab is used to solve (10). Since the split-bus contingency is at Sub. 3, the Lasso solution is expected to reveal nonzeros for the CB-flow states corresponding to any of the five breakers in Sub. 3.

Table 1
Measurement errors in the 13-bus BB model.

Meas. Type	From Bus	To Bus	Meas. (pu)	Est. (pu)	Res. (pu)	Norm. Res.
Real Flow	3	7	−0.950	0.240	−1.010	**177.2**
Real Flow	3	4	0.778	0.741	0.548	**98.4**
Real Flow	1	3	0.811	3.710	−0.510	**82.8**
Real Flow	4	5	0.267	−0.739	0.519	**82.3**

Table 2
Lasso solution for the 13-bus NB model.

No. of Nonzeros	5	4	2	0
Lambda (λ)	0.018	0.020	0.029	0.032
States	Nonzeros Identified			
V. Ang. Bus 3044 (Sub. 7)	−0.0100	−0.0083	0.0	0.0
V. Ang. Bus 3028 (Sub. 3)	0.0100	0.0083	0.0	0.0
V. Ang. Bus 3033 (Sub. 2)	0.0002	0.0	0.0	0.0
CB-flow 3-3026 (Sub. 3)	−0.1749	−0.1521	**−0.0363**	0.0
CB-flow 3-3028 (Sub. 3)	0.2497	0.2140	**0.0363**	0.0

Four different Lasso solutions are shown in Table 2. Going from left to right, the λ value is increased to reduce the number of nonzeros. The λ value is large enough in the last column to force all states to zero. As seen in the second to last column, only the nonzeros corresponding to the CB flows in Sub. 3 remain. Therefore, the location of the topology error is identified as Sub. 3.

As described in Section 4, the Lasso solution is effective in identifying the suspect substation, but further processing is necessary to figure out which breakers tripped/closed. Since the problem substation is already localized based on the Lasso solution, LAV SE is run for the small network (built by including the two-tier neighbors of Sub. 3). This post-processing step is computationally insignificant as only a small number of nodes and a few substations constitute the localized system.

Table 3
CB Status Errors in the 13-Bus NB Model.

From Bus	To Bus	Norm. Flow	Status Decision
3015	10	2.119	Open
3	3026	0.880	**Open**
3027	3025	1.189	Open
3028	3025	1.192	**Open**

Table 4
Lasso solution for the 300-bus NB model.

No. of Nonzeros	4	2	1
Lambda (λ)	0.0020	0.0022	0.0035
States	Nonzeros Identified		
CB-flow P 3679-3680 (Sub. 175)	−0.0729	−0.0618	0.0
CB-flow P 3680-3681 (Sub. 175)	−0.0053	0.0	0.0
CB-flow P 3681-175 (Sub. 175)	−0.1732	−0.1620	−0.0995
CB-flow Q 3681-175 (Sub. 175)	−0.0085	0.0	0.0

As the system size gets larger, the error localization becomes more crucial to eliminate the need to run SE on the whole NB model.

After running LAV SE, the normalized CB-flow test, as described in [18], is used to determine CB open/closed statuses. As shown in Table 3, only the statuses of four CBs in the localized system are identified as erroneous per the normalized CB-flow test, as their normalized flows are less than the open/closed threshold of 3.0. When a closed CB is flagged as open based on the normalized flow test, it means either the breaker is open or negligible amount of current is flowing through it. For CBs 3015-10 and 3027-3025, the latter is true, but even if they are flagged as open, this does not have any material effect on the SE solution. On the other hand, as CBs 3-3026 and CB 3028-3025 correspond to the split-bus contingency, they correctly identify the topology error.

5.2. *Localization of topology errors in large systems*

In a small system like the 13-bus system, it is computationally feasible to run full SE using NB models at each measurement scan. In contrast, to show the benefit of the proposed Lasso procedure for large systems, the NB version of the IEEE 300-bus system offers a more challenging but realistic test case. The NB version of the IEEE 300-bus system, available in IEEE DataPort [24], is used for the proposed algorithm. The conversion from the BB model to NB model is achieved by adding two CBs at the termination of each line, creating either double-bus-double-breaker, ring-bus or breaker-and-a-half substation configurations. The total node count increases to 1233 after adding 1186 CBs.

A split-bus contingency is simulated in Sub. 175 by opening two breakers: CB 3679-3680 and CB 3683-175. The substation configurations showing the split-bus contingency is given in Fig. 5. Assuming this topology change develops between two measurement scans, the Lasso formulation in (10) should reveal nonzeros corresponding to CB-flow states in Sub. 175.

The results of the Lasso solutions are given in Table 4. Since all the nonzeros correspond to the CB-flow states in Sub. 175, the location of the split-bus contingency is correctly identified.

Next, neighbors of Sub. 175 need to be incorporated similar to the illustration in Fig. 2. Matlab's "graph" function is used to create a connection graph of the IEEE 300-bus system in Fig. 6. The shaded region consists of Sub. 175 and its two-tier neighbors (colored in red). This reduced system consists of only 82 buses and 73 CBs compared with the full system with 1233 buses and 1186 CBs. Therefore, running an additional SE cycle on the localized system is computationally trivial.

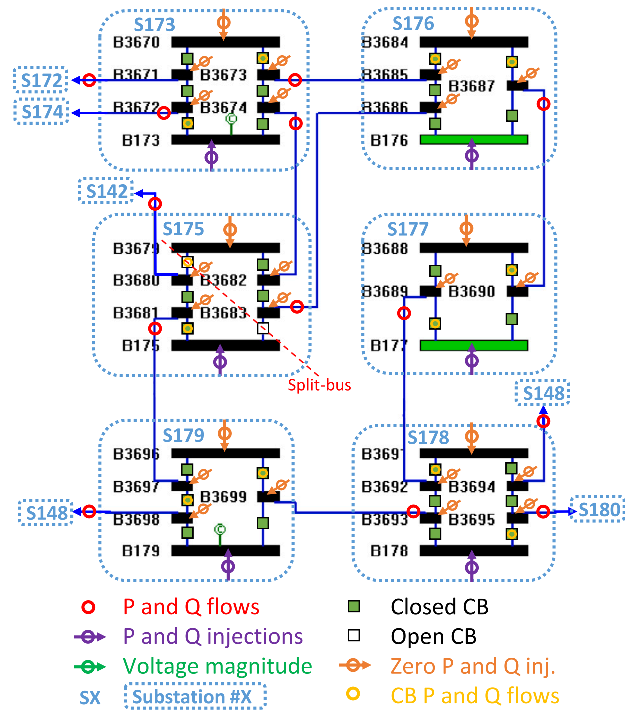

Fig. 5. Split-bus contingency at Substation #175 in the IEEE 300 bus system.

Table 5
CB status errors in the 300-bus NB model.

From Bus	To Bus	Norm. Flow	Status Decision
3679	3680	0.418	**Open**
3679	3682	0.418	Open
3683	175	0.453	**Open**

LAV SE and the subsequent normalized CB-flow test are run for the reduced network. The list of topology errors per the normalized CB-flow test is given in Table 5. The first and third rows show normalized flows less than 3 standard deviations indicating those breakers should be open. Thus, the split-bus contingency is correctly identified. In addition, the flow through CB 3679-3682 comes under the "closed" threshold. Since Bus 3679 is a zero-injection bus, no current would flow through this breaker after CB 3679-3680 trips as part of the split-bus contingency. Therefore, its normalized flow is below the closed threshold.

6. Conclusion

A computationally efficient procedure to track changes in the network topology is developed in this paper. It is shown that commonly used bus-branch equivalents cannot represent complex topology changes until topology processor updates the network. In case of delays or errors in topology processing, the accuracy of SE is jeopardized. To overcome this shortcoming, a method that utilizes node-breaker models is formulated. The detection of topology errors is accomplished through a two-step process. First, the Lasso method is employed to identify if any substations experienced topology changes from one measurement scan to the next. Once the location of the topology error is identified, a reduced network around the suspect substation is formed. It is shown that running SE for this reduced network is sufficient to reveal the correct breaker statuses. The proposed method is verified both in a small system with 13 substations and a large system with 300 substations. Analysis of more complex contingencies (e.g., stuck breakers) that can split the system into several observable islands is

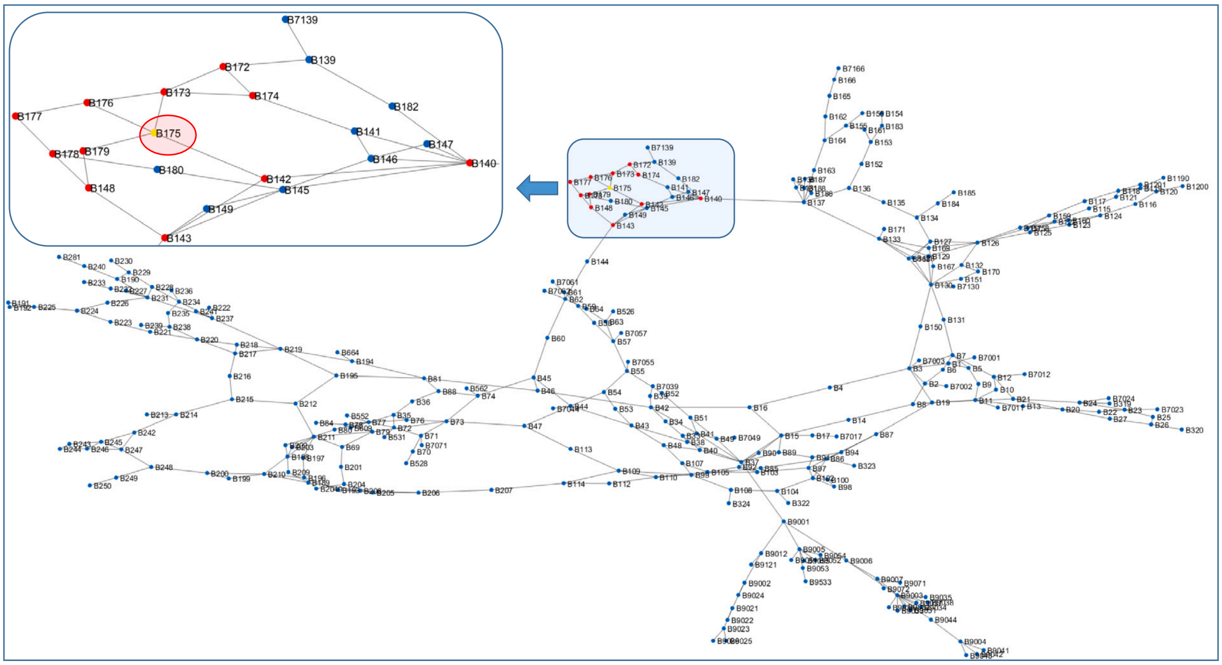

Fig. 6. Substation connection graph for the IEEE 300 bus system.

left as future work. In addition, since the Lasso method is suitable for underdetermined systems, the efficiency of the proposed method when only a subset of measurements is available will be evaluated.

CRediT authorship contribution statement

Bilgehan Donmez: Data curation, Methodology, Writing – original draft, Software, Visualization. **Ali Abur:** Conceptualization, Supervision, Writing – review & editing.

Declaration of competing interest

The authors declare that they have no known competing financial interests or personal relationships that could have appeared to influence the work reported in this paper.

References

[1] A.M. Sasson, S.T. Ehrmann, P. Lynch, L.S.V. Slyck, Automatic power system network topology determination, IEEE Trans. Power Syst. PAS-92 (2) (1973) 610–618, http://dx.doi.org/10.1109/TPAS.1973.293764.

[2] M. Prais, A. Bose, A topology processor that tracks network modifications, IEEE Trans. Power Syst. 3 (3) (1988) 992–998.

[3] M.R. Irving, M.J. Sterling, Substation data validation, IEE Proc. 129 (3) (1982) 119–122.

[4] A. Monticelli, The impact of modeling short circuit branches in state estimation, IEEE Trans. Power Syst. 8 (1) (1993) 364–370.

[5] A. Monticelli, Modeling circuit breakers in weighted least squares state estimation, IEEE Trans. Power Syst. 8 (3) (1993) 1143–1149.

[6] A. Abur, H. Kim, M.K. Celik, Identifying the unknown circuit breaker statuses in power networks, IEEE Trans. Power Syst. 10 (4) (1995) 2029–2037.

[7] A. Gómez-Expósito, A. de la Villa Jaén, Reduced substation models for generalized state estimation, IEEE Trans. Power Syst. 16 (4) (2001) 839–846, http://dx.doi.org/10.1109/59.962435.

[8] K.A. Clements, A.S. Costa, Topology error identification using normalized Lagrange multipliers, IEEE Trans. Power Syst. 13 (2) (1998) 347–353.

[9] L. Mili, G. Steeno, F. Dobraca, D. French, A robust estimation method for topology error identification, IEEE Trans. Power Syst. 14 (4) (1999) 1469–1476.

[10] O. Alsac, N. Vempati, B. Stott, A. Monticelli, Generalized state estimation, IEEE Trans. Power Syst. 13 (3) (1998) 1069–1075, http://dx.doi.org/10.1109/59.709101.

[11] G.N. Korres, P.J. Katsikas, G.E. Chatzarakis, Substation topology identification in generalized state estimation, Int. J. Electr. Power Energy Syst. 28 (3) (2006) 195–206.

[12] V. Kekatos, G.B. Giannakis, Joint power system state estimation and breaker status identification, in: Proc. North American Power Symp., Sep. 2012, 2012, pp. 1–6.

[13] E. Andreoli, A.S. Costa, K.A. Clements, Topology validation via simultaneous state topology estimation with phasor data processing capability, in: Proc. Power Syst. Comput. Conf., 2014, pp. 1–7, http://dx.doi.org/10.1109/PSCC.2014.7038474.

[14] V. Freitas, A.S. Costa, Integrated state topology estimation based on a priori topology information, in: Proc. IEEE Eindhoven PowerTech, 2015, pp. 1–6, http://dx.doi.org/10.1109/PTC.2015.7232440.

[15] E.M. Lourenço, E.P.R. Coelho, B.C. Pal, Topology error and bad data processing in generalized state estimation, IEEE Trans. Power Syst. 30 (6) (2015) 3190–3200.

[16] O. Ardakanian, V.W.S. Wong, R. Dobbe, S.H. Low, A. von Meier, C.J. Tomlin, Y. Yuan, On identification of distribution grids, IEEE Trans. Control Netw. Syst. 6 (3) (2019) 950–960, http://dx.doi.org/10.1109/TCNS.2019.2891002.

[17] R. Tibshirani, Regression shrinkage and selection via the Lasso, J. R. Stat. Soc. Ser. B Stat. Methodol. 58 (1996) 267–288.

[18] B. Donmez, A. Abur, Static state estimation without topology processor, IEEE Trans. Power Syst. 36 (5) (2021) 4712–4722, http://dx.doi.org/10.1109/TPWRS.2021.3064975.

[19] H. Singh, F.L. Alvarado, Network topology determination using least absolute value state estimation, IEEE Trans. Power Syst. 10 (3) (1995) 1159–1165.

[20] Y. Lin, A. Abur, Enhancing network parameter error detection and correction via multiple measurement scans, IEEE Trans. Power Syst. 32 (3) (2017) 2417–2425, http://dx.doi.org/10.1109/TPWRS.2016.2608964.

[21] Mathworks, Lasso Or elastic net regularization for linear models, 2021, Available: https://www.mathworks.com/help/stats/lasso.html. [Online]: (Accessed 15 September 2021).

[22] A. Abur, F.H. Magnago, F.L. Alvarado, Elimination of leverage measurements via matrix stretching, Int. J. Electr. Power Energy Syst. 19 (8) (1997) 557–562.

[23] A. Abur, Power Education Toolbox (PET), [online] available: http://www1.ece.neu.edu/~abur/pet.html.

[24] B. Donmez, Node-breaker model of the IEEE 300-bus system, IEEE Dataport (2021) http://dx.doi.org/10.21227/f908-cy10.